Control of replication associated DNA damage responses by Mismatch Repair

Ijsselsteiijn, R.

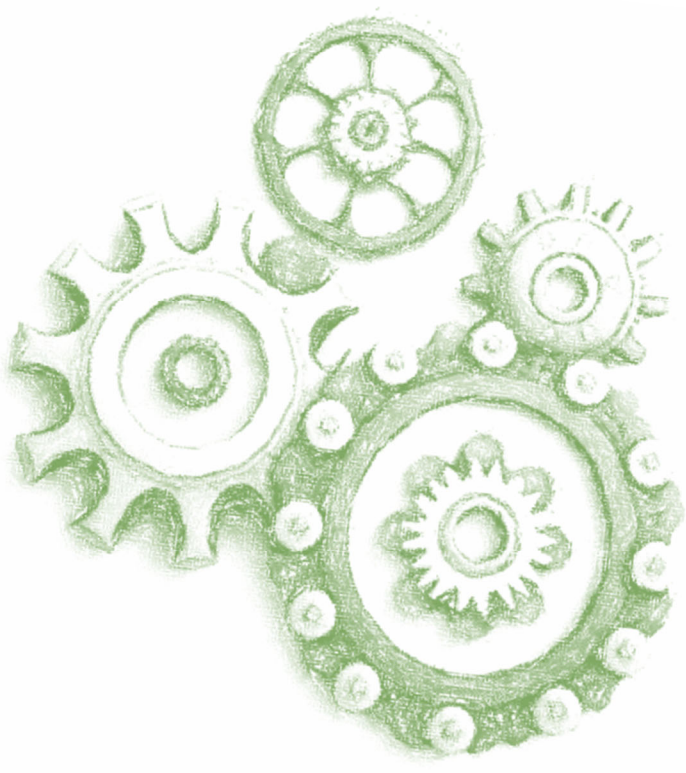

Chapter 4:

Elucidating the genetic entanglement of translesion synthesis and mismatch repair during the ultraviolet light-induced DNA damage response

Robbert Ijsselsteijn[1], Jente Houweling[1], Jacob G Jansen[1]

[1]Department of Human Genetics, Leiden University Medical Center, Leiden, The Netherlands.

Abstract

Translesion synthesis (TLS) is an evolutionary conserved DNA damage tolerance pathway by which low fidelity TLS polymerases replicate across DNA helix-distorting nucleotide lesions. TLS allows completion of genomic DNA replication while quenching DNA damage signaling, thereby promoting cell survival at the expense of mutagenesis. Proteins involved in DNA mismatch repair (MMR) likely play a role in suppressing error-prone TLS. Two models have been described: (i) MMR-mediated recruitment of TLS polymerases to damaged nucleotides and (ii) the removal of TLS-induced mis-incorporations by MMR proteins in a pathway dubbed post-TLS repair. The latter predicts that MMR-dependent control of TLS correlates with the extent of error-prone TLS, while the former predicts an epistatic relationship between MMR and TLS. To distinguish between these two models, we generated mouse embryonic stem (mES) cells defective for Polymerase Eta (Polη), a TLS polymerase that replicates across UV-induced cyclobutane pyrimidine dimers (CPDs) in a relatively error-free fashion. Upon UV exposure, Polη-deficient mES cells display formation of single stranded DNA (ssDNA) gaps opposite CPDs, activation of DNA damage signaling, delayed cell cycle progression and enhanced mutagenesis resulting from increased error-prone TLS. UV-induced mutagenesis is further increased in Polη-deficient mES cells with additional defects in the MMR genes *Msh6* or *Mlh1*. Interestingly, Msh6, but not Mlh1, is required for formation of ssDNA gaps and activation of cell cycle responses in Polη-deficient mES cells. These results agree with Msh6-dependent excision of TLS-induced mis-incorporations opposite UV lesions, resulting in checkpoint activation and suppression of TLS-induced mutagenesis. Mlh1 suppresses UV-induced mutagenesis independent of DNA damage signaling and checkpoint control.

Introduction

Bulky DNA lesions that distort the helix structure of DNA form a strong block for the replicative DNA polymerases delta and epsilon. This blockage leads to stalling of replication forks that activate DNA damage signaling cascades, which contribute to fork stabilization and induce a cell cycle arrest. However, persistently stalled forks ultimately collapse, resulting in the formation of double stranded DNA breaks (DSB), gross genomic instability and cell death. To prevent replication fork collapse at helix-distorting DNA lesions, cells activate Translesion Synthesis (TLS), an evolutionary conserved DNA damage tolerance pathway that allows replication across and beyond nucleotide lesions, thereby quenching DNA damage signaling, enabling completion of DNA replication and preventing cell death (1).

Translesion synthesis is performed by a group of TLS polymerases that can be subdivided into two subfamilies: the Y-family DNA polymerases (Polη, κ, ι and REV1) that insert nucleotides opposite the DNA lesion, forming so-called compound lesions, and the B-family DNA polymerase ζ (consisting of the catalytic subunit Rev3 and the accessory proteins Rev7, PolD2 and PolD3), important to extend DNA replication from compound DNA lesions. In contrast to DNA polymerases delta and epsilon, TLS polymerases lack the ability to perform 3'-5' proofreading. Moreover, Y-family polymerases have a more relaxed active site, allowing for the incorporation of

nucleotides opposite DNA lesions. However, the increased flexibility and the loss of proofreading lowers replication fidelity significantly (2). Consequently, replication of damaged DNA by TLS comes at the expense of mutagenesis.

Polη is the only Y family TLS polymerase associated with human disease. Polη is known for the relatively error-free bypass of UV-induced thymine-thymine cyclobutane dimers (CPD) due to its structure that seems uniquely suited to incorporate adenines opposite T-T CPDs (3). Mutations in *PolH*, the human gene encoding Polη, give rise to Xeroderma Pigmentosum Variant (XPV) (4), an autosomal recessive disease, characterized by sensitivity to sunlight and strongly increased susceptibility to skin cancer formation resulting from UV-induced apoptosis and mutagenesis(5). The phenotypes of XPV highlight the two main roles Polη performs in dealing with UV damage, namely efficient, but also relatively error-free bypass of UV-induced CPD lesions. The absence of Polη lowers TLS processivity resulting in replication fork collapse, gross genomic instability and apoptosis. Moreover, compared to Polη, back-up TLS polymerases are more mutagenic opposite UV lesions resulting in increased UV-induced mutagenesis and carcinogenesis (6).

As illustrated by the XPV phenotype, recruiting the 'correct' polymerase to bypass a nucleotide lesion is important to keep the mutagenic effects of TLS as low as possible. Control of mutagenic TLS occurs in multiple ways. Recruitment of TLS polymerases to the nucleotide lesion is a regulated process, which includes the mono-ubiquitination of PCNA, a DNA clamp that acts as a processivity factor for DNA polymerases, thereby enhancing its interaction with TLS polymerases, in particular Polη. How the choice is made between different TLS polymerases for the bypass of various lesions is still a matter of debate, but it is clear that some polymerases will be more accurate on certain lesion types than others (7). Interestingly, replication extension from a Polη-induced mis-incorporation is less efficient than when the correct nucleotide is incorporated (8, 9). Moreover, if Polη halts replication when it mis-incorporates, it may hypothetically allow extrinsic exonucleases to outcompete TLS polymerases and remove the mis-incorporation, thereby controlling TLS mutagenicity. TLS-associated mutagenicity is also reported to be controlled by DNA mismatch repair (MMR). In canonical MMR, a heterodimer consisting of MSH2 and MSH6 (also known as MutSα) is required for the recognition of a base:base mismatch and the MLH1/PMS2 heterodimer (MutLα) for the subsequent nicking of the DNA and promotion of exonucleases that remove the mismatch (10). Several studies have shown that in the absence of MMR, methylation and oxidative DNA damage-induced mutagenicity is no longer suppressed (11-13), indicating that MMR also recognizes and removes mis-incorporations opposite slightly modified bases. Moreover, MMR proteins also suppress the mutagenicity of bulky helix-distorting DNA lesions induced by genotoxic agents such as UV-C light or the dietary mutagen PhIP (14, 15). The control of UV-induced mutagenesis is often accompanied with the formation of ssDNA, resulting in DNA damage signaling, cell cycle responses and apoptosis (16).

Two models are proposed to explain the suppression of UV-induced mutagenesis and DNA damage responses by MMR proteins (Fig. 1). First, the post-TLS repair model suggests that MMR proteins may perform a function reminiscent of canonical MMR, namely to reduce TLS-associated mutagenesis by removing the mis-incorporations opposite damaged DNA (17). This model is supported by the finding that MutSα binds more tightly to compound mismatches compared to correct base:lesion matches (18). Moreover, loss of Msh6 leads to increased UV-induced mutagenicity, reduced formation of ssDNA opposite UV-lesions and reduced levels of DNA damage signaling (17). Second, the role of MMR in suppressing UV-induced mutagenicity may be explained by MMR proteins that bind and recruit TLS polymerases to the lesion site. Some reports indicate that in response to various lesion types this non-canonical (nc)MMR pathway leads to MMR-dependent ubiquitination of PCNA to recruit Polη to the site of damage (19, 20). However, another study suggests that MutSα can recruit Y family TLS polymerases to UV lesions independent of PCNA ubiquitination (21). This model suggests that when MMR is unavailable, Polη and other Y family TLS polymerases cannot be recruited to bypass UV-lesions, thereby affecting UV mutagenesis and damage responses. Moreover, DNA damage signaling and single strand gap formation can possibly also be caused by MutSα-dependent processing of stalled forks (22) or Exo1 hyper-resection (23) as discussed in the chapter 3. These models do not explain the protective role of MMR when dealing with UV-induced mutagenesis and investigating these further falls outside the scope of this work. Similarly, MMR may be able to suppress mutagenicity by inducing DNA damage signaling thus causing cell cycle arrests allowing for DNA repair to take place or steer cells into senescence or apoptosis (24, 25), therefor preventing mutagenesis. In chapter 3, our findings revealed that Mlh1 has a protective effect against UV-induced mutagenesis, independent of the aforementioned damage signaling mechanisms. Hence, these models are unlikely to provide a plausible explanation for the observed suppression of UV-induced mutagenesis.

In this work we set out to study the relationship between TLS Polη and MMR (Fig. 1). In particular, how MMR controls UV/TLS-associated mutagenesis and activates DNA damage signaling resulting in cell cycle arrests and apoptosis in mouse embryonic stem (mES) cells that are deficient for Polη. The nature of the relationship between TLS and MMR could be elucidated by comparing *Polh*-deficient mES cells to *Polh*-deficient mES cells with an additional defect in *Msh6*, together with *Msh2* involved recognition of base-base mismatches, or with a defect in *Mlh1* that acts downstream of MutSα. An epistatic relationship is expected for a recruitment-based model, whereas the post-TLS repair model would be reflected by a synergistic relationship Polη and MMR proteins. Here we show that UV-induced mutagenesis is increased in *Polh*-deficient cells and that additional deficiency for *Msh6* or *Mlh1* further exacerbates UV-induced mutagenesis. Moreover, cell cycle arrests and apoptotic responses in *Polh*-deficient cells depend on *Msh6*, but not on *Mlh1*. In line with this, DNA damage signaling and the formation of ssDNA gaps opposite UV damage only relies on Msh6.

Taken together, these data show a synergistic relationship between Polη and the MMR proteins Msh6 and Mlh1 in support of the post-TLS repair model (26).

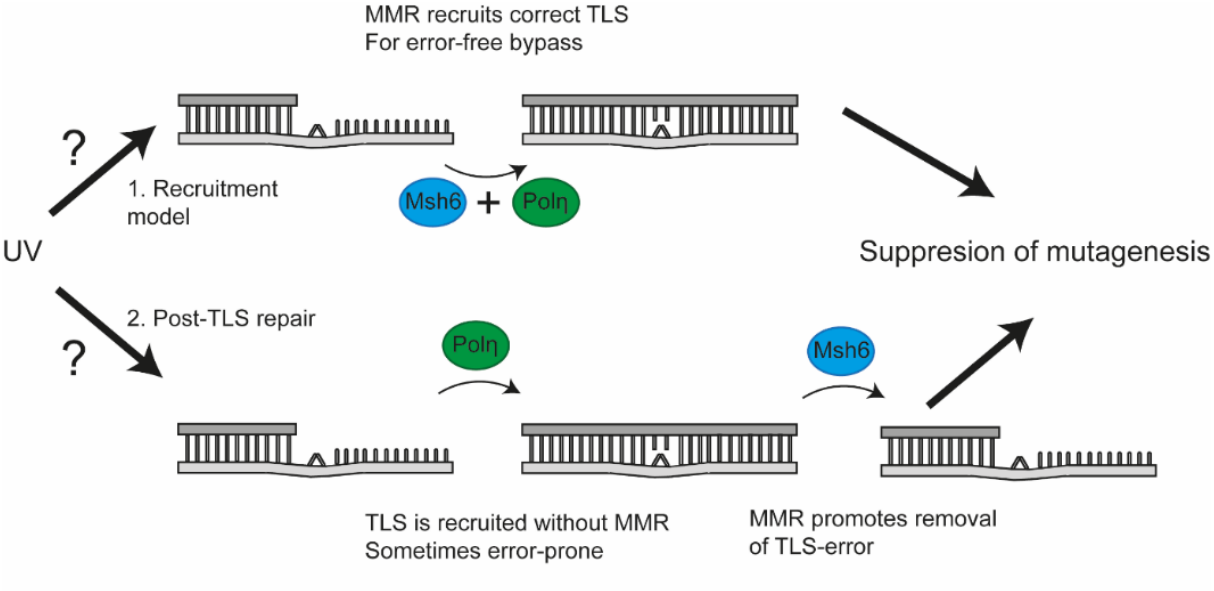

Figure 1: Recruitment and post-TLS repair models
UV radiation introduces DNA lesions (depicted by the crossed nucleotide bars) that cannot be bypassed by replicative polymerases. Polη is recruited as a relatively error-free TLS polymerase to replicate across the damaged DNA. Two models are proposed to reduce mutagenicity of UV lesions: 1) recruitment of Polη instead of more error-prone TLS polymerases by MMR proteins or 2) post-TLS repair, the post-replicative removal by MMR proteins of mis-incorporated nucleotides opposite DNA damage.

Materials and Methods

Mouse embryonic stem cell culture and cell lines

The generation of the wild-type mouse embryonic stem (mES) cell line is described elsewhere (27). This wild-type cell line was used as a parental cell line to generate all other cell lines in this work. The generation of the Msh6 single mutant cell line is described elsewhere (28). Cells were made deficient for *Polh* using CRISPR/Cas9 with guideRNAs targeting both the 5' and 3' region of the *Polh* gene (Supplemental methods table 1). Two independent *Polh*-deficient lines were generated which were validated by two genomic PCR strategies (Fig. 2, supplemental methods table 2). These cell lines were used for the generation of independent *PolhMsh6* and *PolhMlh1* double knockout cell lines using CRISPR/Cas9 (Supplemental methods table 1). After transfection with CRISPR/Cas9 expression constructs, the cells underwent an additional treatment with 40μM 6-thioguanine (6tG) for four hours to select for MMR

deficiency, which was validated on western blot (Abcam, clone 44, C-20, Santa Cruz Biotechnology for Msh6 and Mlh1, respectively). mES Cells were cultured on gelatin-coated dishes in “complete medium” which consisted of DMEM KO (Gibco) supplemented with 10% fetal calf serum (Bodinco/Capricon Scientific), 0.1mM β-mercaptho-ethanol (Sigma-Aldrich), 1mM pyruvate (Gibco), 1% non-essential amino acids (Gibco), 1% glutamax (Gibco), 100U penicillin/ 100µg streptomycin (Gibco) and leukemia inhibitory factor (made in house).

Determination of UV-induced mutagenicity

Msh6, *Polh*, *PolhMsh6* and *PolhMlh1* deficient cells as well as WT cells were treated with 5mM Hypoxanthine, 20µM Aminopterin, 0.8µM Thymidine (HAT, 50x diluted, Thermo Fisher Scientific) for 6 days and afterwards with 5mM Hypoxanthine, 0.8µM Thymidine (HT, 50x diluted, Thermo Fisher Scientific) for 2 days to select for cells with functional Hprt. Next, 5 million cells per p90 culture dish were seeded and grown for a day before being exposed to 2J/m^2 of UV-C or mock treated. After treatment, the cells were maintained for 6 days before being seeded in a cell density of $4x10^5$ per p90 (5 p90 dishes per cell line) in the presence of 30µM 6tG to select for clones that have lost *Hprt*. From the same cell suspensions, 250 cells were seeded in 3 p60 culture dishes to determine the cloning efficiency of the cells. After 7-10 days the clones were stained using methylene blue and the *Hprt* mutant frequency was determined by counting the 6tG-resistant clones while adjusting for the cloning efficiency of cells.

Determination of cell cycle progression and apoptosis by FACS

Two million WT, *Msh6*, *Polh*, *PolhMsh6* and *PolhMlh1*-deficient cells were seeded in a p60 culture dish one day prior to exposure to 2J/m^2 of UV-C or mock treatment. After treatment, cells were incubated in medium containing 10µM BrdU (Merck Millipore) for 30 minutes and subsequently chased in medium containing 5µM thymidine (Invitrogen) until the timepoint was reached. Next, cells were trypsinized and added to the medium in which the cells were cultured. Cells were pelleted by centrifugation and fixed in ice cold 70% ethanol. For BrdU staining cells were pelleted and permeabilized/denatured using 0.5% Triton X-100 (Sigma Aldrich) in 2M HCL for 35 minutes at RT. The mixture was neutralized by adding an excess of 1M Tris (Sigma Aldrich). After centrifugation, the cells were washed once with PBS containing 0.5%Tween-20 + 5% Fetal Calf Serum (PBS-TS). Next, cells were incubated in 20µl mouse monoclonal anti-BrdU antibody (B44, BD Biosciences) and 30µl PBS-TS at 4^0C for overnight. Afterwards, the cells were washed with PBS-TS and incubated with FITC-conjugated rat-anti-mouse antibody (1: 62.5, BD Pharmingen) diluted in PBS-TS for one hour in the dark. Finally, the cells were washed with PBS-TS and incubated using PBS containing propidium iodine (10µg/ml, Sigma Aldrich) and RNAse A (100µg/ml, Roche Diagnostics). Cells were analyzed using a Novocyte Fluorescence Activated Cell Sorter (Acea

Biosciences) using gates for PI versus GFP. The different cell cycle phases as well as the apoptotic fraction was determined as described in supplementary figure S3.

Analysis of UV-induced DNA damage signaling

One million *Polh*, *PolhMsh6* and *PolhMlh1* deficient cells were seeded per well of a 6-wells plate one day prior to treatment. Cells were treated with 2J/m^2 of UV as described above and incubated in complete medium for different times. Cells were lysed in 250µl 2x Laemmli sample buffer. 12.5µl of cell lysate was used for western blot as described above. Primary antibodies against Kap-1^p (1:1000, Bethyl, polyclonal A300-767A) and Chk1^p (1:1000, Cell signaling technology, clone 133D3) were used to measure DNA damage signaling, antibodies against PCNA (1:8000, Santa Cruz, clone PC10) were used as a loading control. Antibodies against Msh6 (1:250, Abcam, clone 44) and Mlh1 (1:1000, Santa Cruz, polyclonal C20) were used for knock-out validation.

Determination of chromatin-bound Rpa

Polh, *PolhMsh6* and *PolhMlh1*-deficient cells were seeded in a cell density of 1.5x10^6 cells per p60 culture dish, one day prior to irradiation with UV. Then, the cells were washed once with PBS and exposed to 2J/m^2 of UV-C. After exposure, the cells were incubated for 0 or 4 hours in complete medium. The cells were collected by trypsinization and 2 million cells were fractionated using a Subcellular Protein Fractionation Kit for Cultured Cells (Thermo Fisher Scientific) according to manufacturer's protocol. The total amount of protein in each fraction was measured using a Bradford assay (Thermo Fisher Scientific). Thirty µg of chromatin-bound protein extract was analyzed by western blot . Proteins were size-separated in 4-12% Criterion XT Bis-Tris Gels (Biorad) by gel electrophoresis using 70V for two hours followed by 120V for two hours. Next, the proteins were transferred onto 0.45µM nitrocellulose membranes (Protran, GE Healthcare) using 400mA (~70V) for two hours or at 200mA for overnight at 4°C. Protein membranes were incubated with Rockland blocking reagent (Rockland) diluted 1:1 with 0.1% PBS-tween (Rockland-PBS-T) for 1 hour at RT. Then, membranes were incubated in mixtures of Rockland-PBS-T containing primary antibodies against Histone H3 (1:14000, Abcam, polyclonal) and RPA (1:1000, Cell signaling technology, Clone 4E4) for overnight at 4°C. The membranes were washed with PBS-T and incubated with a mixture containing Rockland-PBS-T and secondary anti-mouse and anti-rabbit HRP antibodies (1:50000, Thermo Fisher Scientific) for one hours at RT. Membranes were washed again using PBS-T and the protein bands were subsequently visualized using Amersham ECL select (GE Healthcare).

Quantification of CPDs in ssDNA

One day prior to UV irradiation 5 x10^6 *Polh*, *PolhMsh6* and *PolhMlh1* deficient cells were seeded in complete medium in p90-culture dishes. Cells were exposed to 2J/m^2 UV-C and incubated in complete medium containing 10µM EdU (Sigma Aldrich) for 30 minutes. Next, medium containing EdU was aspirated, and cells were incubated in medium containing 5µM Thymidine (Invitrogen) for 3.5 hours. For the 0 timepoints,

EdU labeling was done prior to UV-exposure. Subsequently, cells were collected by trypsinization, pelleted by centrifugation and washed with PBS, before incubation in ice cold CSK-Triton buffer (100 mM NaCl, 300 mM sucrose, 3 mM $MgCl_2$, 10 mM PIPES, 0.5% triton X-100, pH 7.2 – 7.5) for 2 minutes on ice. Afterwards, 10 ml PBS is added, cells are pelleted by centrifugation and fixed using 4% paraformaldehyde (Merck Millipore) for 20 minutes at RT. Finally, the cells were washed once more using PBS and pelleted before being resuspended in 1ml PBS. Using a cytospin (Cytospin 4, ThermoScientific) the cells were centrifugated onto KP frost glass slides (Klinipath) and fixed onto the slides using 4% formaldehyde (Klinipath). Slides were stored in PBS until use. EdU stain was performed using Click-iT EdU Cell Proliferation Kit for Imaging 488 Dye (Thermo Fisher Scientific) following manufacturer's protocol. Afterwards, the cells were blocked in PBS containing 3% Bovine Serum Albumin (BSA) (Sigma Aldrich) and 0.1% Tween-20 (Sigma Aldrich) for 30 minutes. The slides were incubated with anti-CPD primary antibodies (1:1000, clone TDM-2, Cosmo Bio) in the dark for overnight at 4^0C. Cells were then washed with five times with PBS-0.1% Tween-20 and incubated with secondary alexafluor-555 antibodies (1:1000, Thermo Fisher Scientific) for 1 hours at RT in the dark. After three times washing with PBS-0.1% Tween-20 and once with PBS, cells were mounted in anti-fade mounting medium containing DAPI (Vectashield). Cells were imaged using an AxioImagerM2 microscope (Zeiss) at 40x magnification. Quantification of integrated density was performed using ImageJ 2.1.0. The EdU-channel was binarized using the default threshold and used as a mask for the quantification of the integrated density of the CPD channel. Individual cells sized between 0.5 and 2.5 $inch^2$ were analyzed.

Results

Pol Eta deficiency: a model to study control of TLS-induced mutagenesis by MMR

Previously, MMR has been shown to reduce mutagenesis resulting from nucleotide lesions possibly by controlling TLS-associated mis-incorporations (29-31). How MMR regulates TLS fidelity has yet to be fully elucidated, but two main hypotheses are studied in this work (Fig.1): (1) MMR proteins recruit the "correct" TLS polymerases to the DNA damage (recruitment model) or (2) post-replicative removal by MMR proteins of TLS-induced mis-incorporations, dubbed post-TLS repair (17, 19-21). In this work we addressed these possibilities by generating mouse ES cells deficient for TLS *Polh* with or without an additional defect in *Msh6* or *Mlh1*. *Polh* acts relatively error-free at UV-induced CPD lesions compared to the other TLS polymerases (32). Therefore, *Polh* deficient cells are more mutable by UV-light, which allows us to more accurately study TLS-associated mutagenesis. Wild-type mES cells were made *Polh*-deficient by deleting the complete *Polh* gene using CRISPR/Cas9-induced DNA breaks at the 5' and 3' ends of the gene (Fig. 2A). We created two independent *Polh*-deficient clones as validated by a PCR using a primer pair that generates PCR fragments only when the entire gene is removed, whereas no PCR fragment was found using a primer pair that creates a PCR fragment when the gene is still present (Fig. 2B). Using CRISPR/Cas9 in combination with a positive selection for MMR-deficiency, 6TG, we

obtained *PolhMsh6* and *PolhMlh1* double knock-out clones in both *Polh*-deficient cell lines (Fig. 2C).

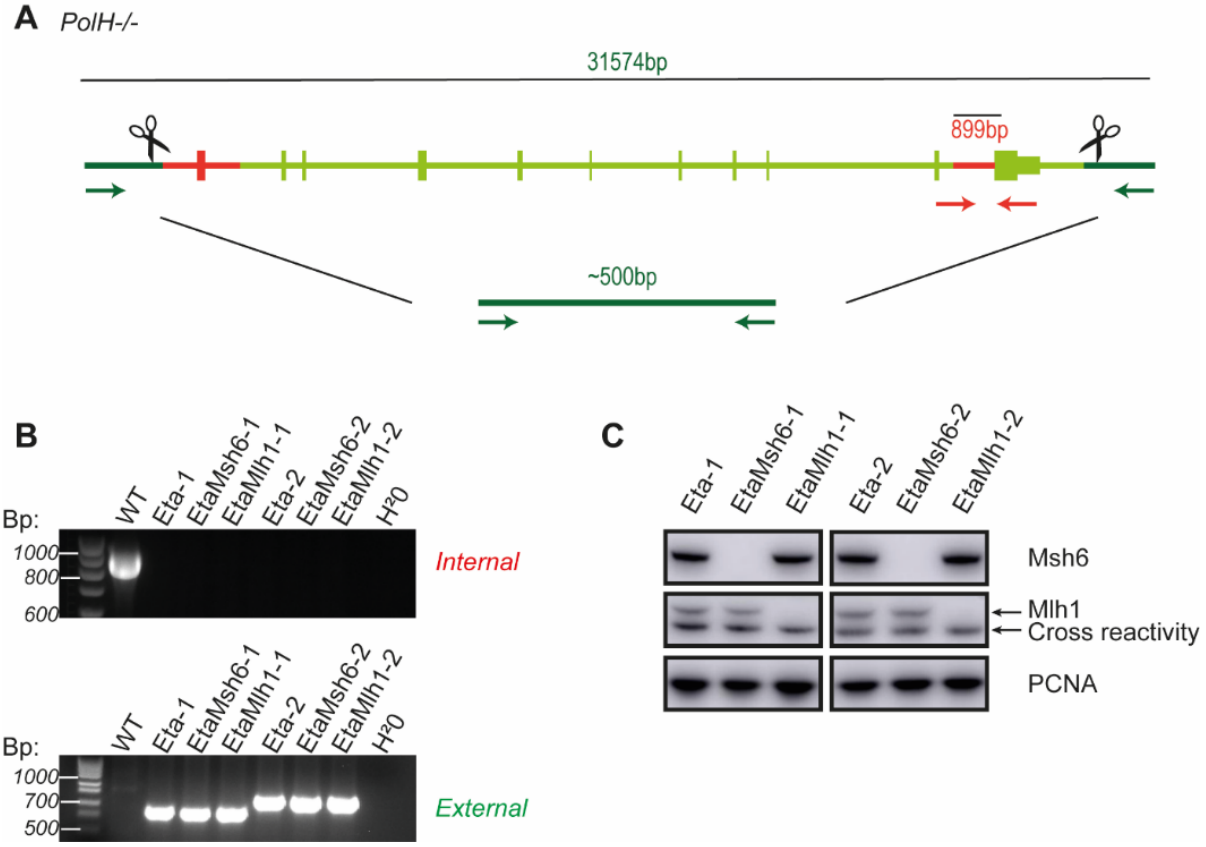

Figure 2: Generation of Polη-deficient cell lines
A: *Polh*-deficient cell lines were generated using CRISPR/Cas9 with guideRNAs (depicted as scissors) directing the cut slightly before and after the gene. Two sets of primers were designed to assess knock-out: a pair that targets a part of the gene to be deleted (external, red arrows) and a pair that targets the area outside of both sides of the gene (internal, green arrows). B: PCR on DNA level with the internal primer pair that is predicted to produce a 899bp product (if knock-out was unsuccessful) and a PCR with the external primer pair predicted to produce a product of approximately 500bp depending on the deletion size and method of repair (if knock-out is successful). C: Western blot was used to validate knock-out of *Msh6* and *Mlh1* in *Polh*-deficient cell lines.

Mutagenicity from UV-induced TLS-errors is controlled by both Msh6 and Mlh1

To elucidate how MMR controls TLS-associated mutagenesis, we exposed wild-type, *Msh6*, *Polh* and *PolhMsh6* double knockout cells to UV light and determined the frequency of 6tG-resistant clones, a measure for inactivating mutations at the X-linked *Hprt* gene. If MMR controls UV mutagenesis according to the recruitment model, additional knock-out of *Polh* in *Msh6* deficient cells would lead to an epistatic effect on UV mutagenesis, since the “correct” TLS polymerase is no longer recruited upon

inactivation of Msh6. However, in the post-TLS repair model a synergistic effect is expected between an increase of TLS-errors, due to inactivation of *Polh*, and lack of post-replicative control following *Msh6* deficiency (Fig. 1). First, we confirmed that Polη acts as a relatively error-free TLS polymerase at UV lesions as is described in literature (32) by subjecting wild type and *Polh*-deficient mES cells to mock and UV treatments and determine the frequency of *Hprt* mutant clones. Both cell lines show hardly any *Hprt* mutant clones following mock treatment. As expected for a role of Polη in error-free TLS at UV lesions, *Hprt* mutagenesis is higher in *Polh*-deficient cells than in wild-type cells (170.0 x 10^6 versus 81.2 x 10^6) following UV exposure (Fig. 3A, Fig. S1A). We also confirmed the control of UV/TLS-induced mutagenesis by Msh6 (14) by determining *Hprt* mutagenesis in wild-type and *Msh6*-deficient cells following mock treatment and exposure to UV. As expected, mock-exposed *Msh6*-deficient cells display increased spontaneous mutagenesis compared to wild-type cells (192.1 x 10^6), due to loss of canonical MMR in *Msh6*-deficient cells. Following UV exposure, *Hprt* mutagenesis is strongly enhanced in *Msh6*-deficient cells, whilst in WT cells only a minor increase is observed (414.7 x 10^6 vs 81.2 x 10^6). The share of UV-induced mutagenesis, calculated by the subtraction of mutations found in the mock-exposed condition from the UV-exposed condition, is in *Msh6*-deficient cells much higher than in wild-type cells (78.2 x 10^6 vs 222.7 x 10^6) (Fig. 3B, S1B), supportive for a role of Msh6 in controlling UV-induced mutagenesis (14). Finally, we determined UV mutagenesis in *Polh* and *Msh6* double knock-out cells and found that the frequency of UV-induced *Hprt* mutants in these cells is even higher than in *Msh6* single knock-out lines (Fig. 3C-D, Fig. S1 C-D), suggestive of synergism, rather than of epistasis, between *Polh* and *Msh6*. Interestingly, knock-out of *Mlh1* in a *Polh*-deficient background showed a similar response as *PolhMsh6*-deficient cells, suggesting that UV-induced mutagenicity is not only suppressed by Msh6, but also by Mlh1. These data show that there is a positive correlation between the extent of TLS-errors and the protection from mutagenesis by MMR, in support of the post-TLS repair model.

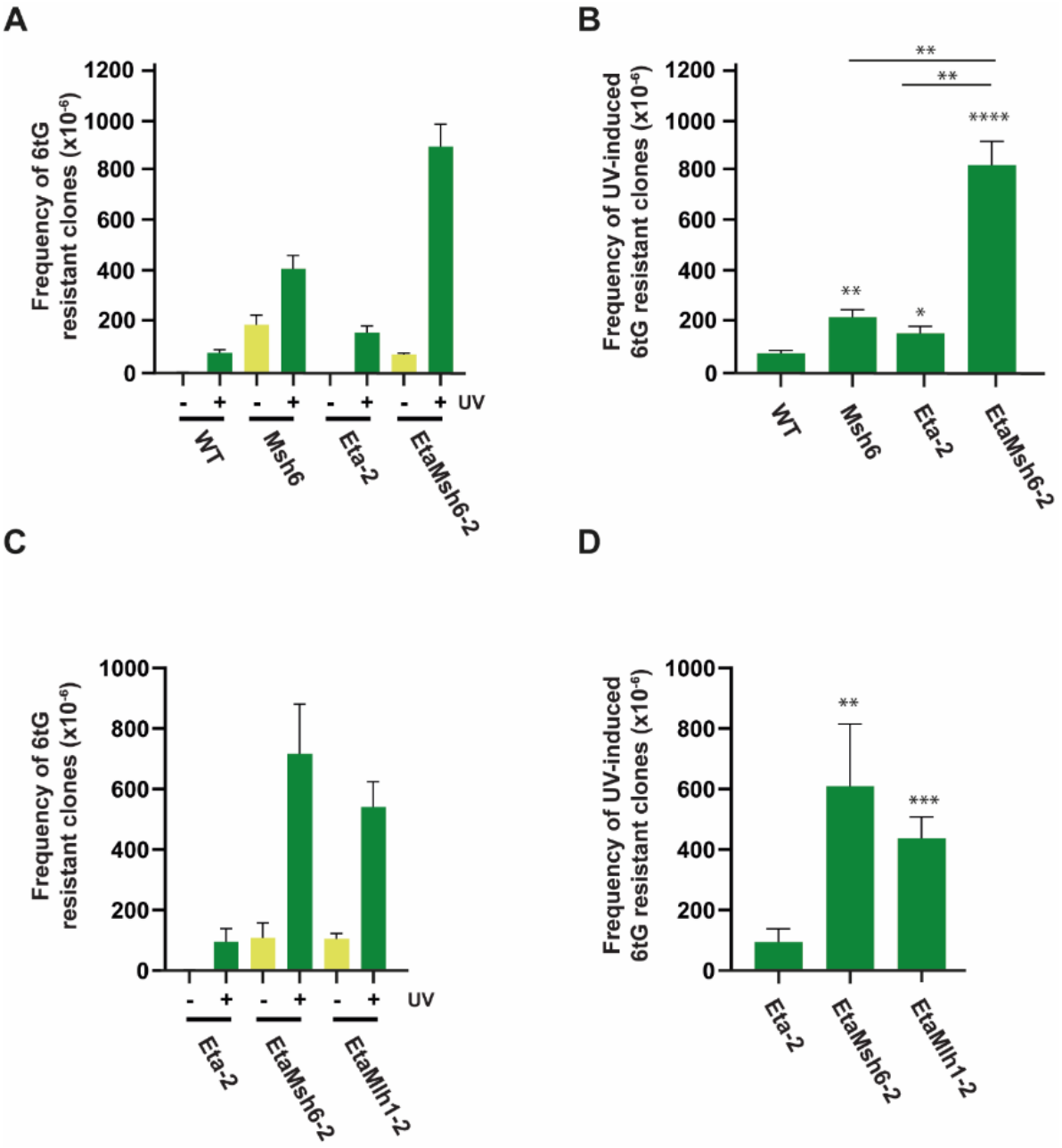

Figure 3: Mutagenicity of error-prone TLS opposed UV-damage is suppressed by Msh6 and Mlh1
A: Frequencies of 6tG-resistant clones containing inactivating Hprt mutations in spontaneous and UV-exposed WT, Msh6, Polη and PolηMsh6-deficient cells. Frequency of 6tG-resistant clones was plotted per million clone forming cells. B: Frequencies of UV-induced 6tG resistant clones in WT, Msh6, Polη and PolηMsh6-deficient cells shown per million clone forming cells. UV-induced mutagenesis was calculated by subtracting mutant frequencies of mock treated cells from those of UV-exposed cells. C: Mutagenesis in mock and UV- exposed conditions, as measured by the frequency of 6tG-resistant clones in Polη, PolηMsh6 and PolηMlh1-deficient cells shown per million clone forming cells. D: UV-induced mutagenesis as calculated by the subtraction of spontaneous mutagenesis from the mutagenesis in UV-exposed conditions in Polη, PolηMsh6 and PolηMlh1-deficient cells shown per million cells. Error bars, SEM; *, P ≤ 0,05; **, P ≤ 0,01; ***, P ≤ 0,001; ****, P ≤ 0,0001; ns, non-significant; student T-test of groups compared to WT or Polη single mutant or between EtaMsh6 and single mutants.

UV-induced cell cycle arrest and apoptosis is aggravated during error-prone TLS and requires Msh6, but not Mlh1

Suppression of UV-induced mutagenesis by MutSα is shown to be accompanied by delayed cell cycle progression due to intra-S checkpoint activation (17), which might be the result of the generation of single stranded DNA (ssDNA) tracts due to excision of TLS-induced 'mis-incorporations' opposite UV lesions. To investigate whether MutSα is required for an UV-induced cell cycle delay in *Polh*-deficient cells, cell cycle progression of BrdU pulse-labelled wild-type, *Msh6*-deficient, *Polh*-deficient and *PolhMsh6* doubly deficient cells was determined by FACS. As a readout we quantified the proportion of BrdU positive cells in G1/early S phase*, i.e*. cells that were replicating at the time of UV exposure or mock treatment and progressed to the subsequent cell cycle. Cell cycle progression of wild-type, *Msh6*-deficient, *Polh*-deficient and *PolhMsh6* doubly deficient cells was similar when these cells are mock-exposed (Fig. S2A-B), whereas UV exposure resulted in delayed cell cycle progression in all genotypes. However, wild-type cells and, in particular, *Polh*-deficient cells progressed much slower through the cell cycle than *Msh6*-deficient and *PolhMsh6* doubly deficient cells (Fig. S2C; compare 8 hours after UV with mock). Moreover, cell cycle progression of UV treated *Msh6*-deficient and *PolhMsh6* doubly deficient cells was almost indistinguishable from mock treated cells. These data not only confirm previous observations (11), but also strongly indicate that MutSα is essential for checkpoint activation in *Polh*-deficient cells following UV exposure. Since both *Msh6* and *Mlh1* protect *Polh*-deficient cells from UV mutagenesis to nearly the same extent (Fig. 3C, D), we wondered if *Msh6* and *Mlh1* play similar roles in UV-induced checkpoint activation. Similar to single knock-out cells, no difference in cell progression was found between double knock-out cell lines and the parental Polη cell lines when not exposed to UV (Fig. S3A-B). However, in stark contrast to loss of *Msh6* in *Polh*-deficient cells, deletion of *Mlh1* in *Polh*-deficient cells showed a similar or even stronger cell cycle block than *Polh* single knockout cells after UV (Fig. 4A-B). By examining the sub-G1 fraction of the cell cycle profiles we could also investigate UV-induced toxicity, as the sub-G1 cells contain a smaller amount of total DNA, which is indicative of apoptosis. Here, we show that *Polh*-deficient cell populations contain a significant fraction of apoptotic cells, starting 16 hours after UV and increasing further 24- and 32-hours post-UV (Fig. 4C, Fig. S3C). Loss of *Msh6* in *Polh*-deficient background rescues this UV sensitivity to wild-type levels at all timepoints. In contrast, *PolhMlh1* lines phenocopy the *Polh* single knock-out line and display *Polh* levels of apoptotic cells after UV-irradiation. These data show that Msh6, but not the downstream MMR factor Mlh1, is required for UV-induced cell cycle arrest and apoptosis.

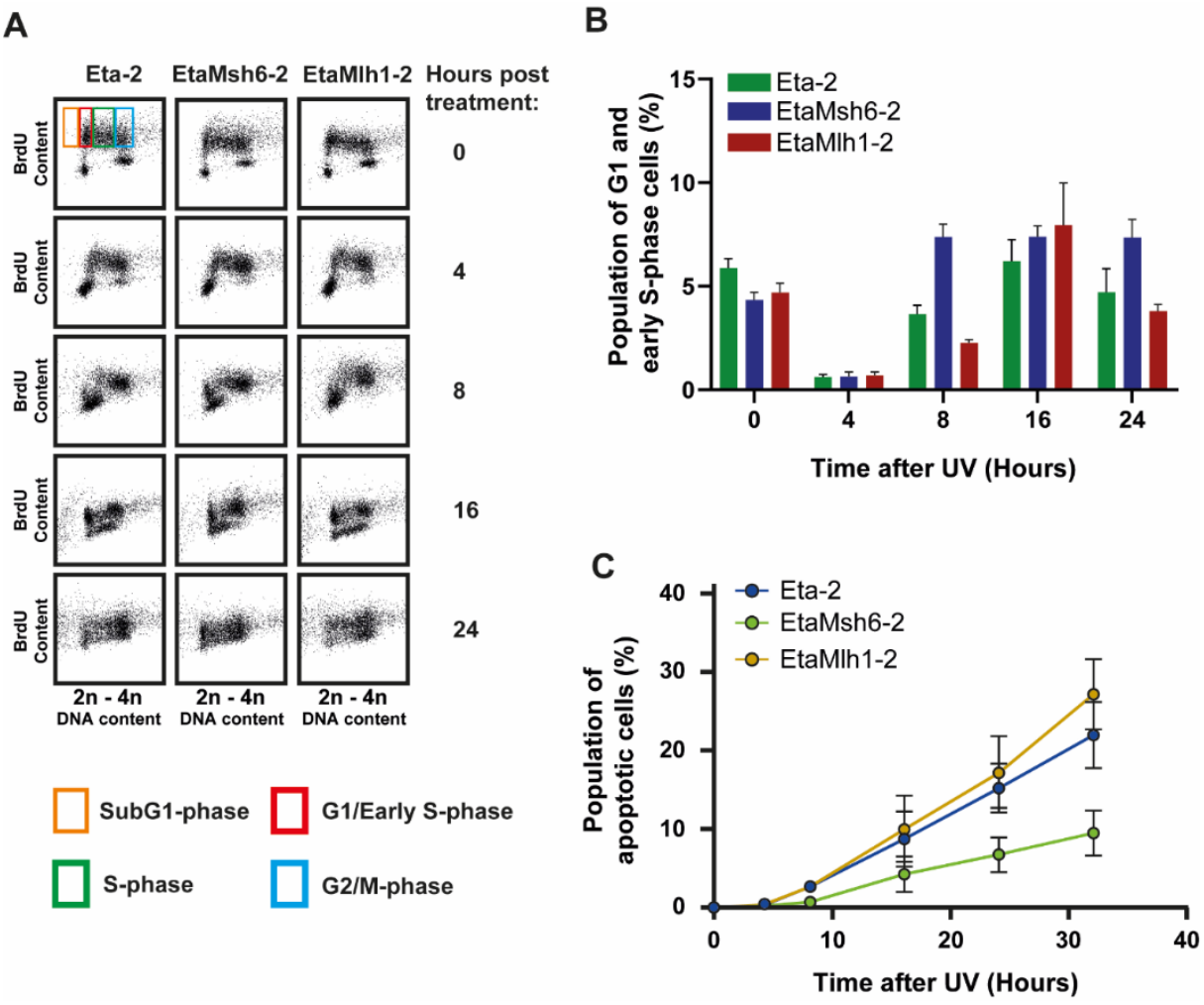

Figure 4: UV-induced cell cycle arrest and apoptosis is dependent on Msh6
A: Cell cycle profiles of Polη, PolηMsh6 and PolηMlh1-deficient cells pulse labeled with BRDU and analyzed for DNA content and BrdU content by FACS 0-24 hours after UV-exposure. B: Quantification of the mean population of G1/Early S-phase cells relative to the total amount of cells in Polη, PolηMsh6 and PolηMlh1-deficient cells, 0-24 hours post-UV. C: Quantification of the mean population of sub-G1 cells relative to the total amount of cells, 0-32 hours post-UV irradiation in Polη, PolηMsh6 and PolηMlh1-deficient conditions. Error bars, SEM.

UV-induced checkpoint responses and ssDNA formation in Pol Eta-deficient cells rely on Msh6

So far Msh6 and Mlh1 control UV mutagenesis in *Polh*-deficient cells to a similar extent, while differently affecting cell cycle progression. To better understand this difference, we focused on the studying the signaling cascade that underlies the UV-induced cell cycle delay. This signaling cascade is thought to start with ssDNA formation and subsequent activation of the signaling kinase Atr/Atrip that phosphorylates a multitude of effector proteins including Chk1, which (i) controls late replication origin firing and elongation of DNA replication, (ii) stabilizes stalled replication forks and (iii) activates the G2/M checkpoint (26). Similarly, Kap-1 is phosphorylated by Atr, however, Kap-1

is also phosphorylated by Atm and as such can be used as a read-out for DSB formation (33-35). Thus, phosphorylation of Chk1 (pChk1) and of Kap-1 (pKap-1) was studied using western blot on whole protein cell extracts obtained from cells, 0, 2, 4 and 8 hours after UV exposure. Nearly undetectable levels of pChk1 and pKap-1 were observed immediately after UV exposure in *Polh*-deficient cells and MMR-deficient derivates thereof (Fig. 5A, Fig. S4A). However, at later timepoints, levels of pChk1 and pKap-1 were clearly increased in *Polh*-deficient cells and this was significantly higher than the increase in the WT parental cell line. The *Msh6* single knock-out cell line nearly abolished all UV-induced signaling, whereas the *PolhMsh6* double knockout showed lower signaling than the *Polh* single knock-out but still markedly higher than the WT cell line (Figure S4A). In contrast, knock-out of *Mlh1* in *Polh*-deficient cells did not affect the ability to activate UV damage signaling, since these cells displayed similar levels and kinetics of pChk1 and pKap1 formation as found in *Polh*-deficient cells after UV exposure (Fig. 5A). To test the possibility that UV damage signaling in *Polh*-deficient and *PolhMlh1* doubly deficient cells relies on the formation of ssDNA rather than on 'direct signaling' by binding of MutSα to compound lesions, *i.e.* a 'mismatched' nucleotide opposite a photolesion (36), we investigated the formation of chromatin-bound Rpa, which coats ssDNA to provide stability. Western blotting revealed that *Polh*, *PolhMsh6* and *PolhMlh1*-deficient cells display similarly low levels of chromatin-bound Rpa, 0 hours after irradiation with UV (Fig. 5B, Fig. S4B). Four hours post-UV, an increase in chromatin-bound Rpa levels was seen in *Polh*-deficient cells, indicating the formation of ssDNA tracts. Additional knock-out of *Msh6* in *Polh*-deficient cells resulted in a strong decrease of chromatin-bound Rpa levels, almost as low as the 0-hour controls. *PolhMlh1* double knockout cells showed an amount of chromatin bound Rpa similar to the *Polh* single knockout.

Msh6-dependent formation of ssDNA gaps opposite CPDs

Previous work indicated that Msh6 may promote excision of misincorporations opposite pyrimidine-pyrimidone (6-4) photoproducts ((6-4)PPs), thus reducing UV-induced mutagenesis. Moreover, using cells that were genetically modified to repair specifically CPDs, it was found that Msh6 not only may act on misincorporations opposite (6-4)PPs but also opposite CPDs (17). Since Polh-deficient cells display enhanced UV mutagenesis (Fig. 3A-B, S1A-B), likely due to more error-prone TLS opposite CPDs, we argued that Polh-deficient cells and MMR-defective derivatives thereof might be a suitable model to determine gap formation opposite CPDs as a read-out for MMR-dependent excision opposite CPDs. Using an antibody that specifically recognizes CPDs in ssDNA conformation (ssCPD), we performed immunostaining under non-denaturing conditions of UV-exposed Polh, PolhMsh6 and PolhMlh1-deficient cells. These cells were pulse labeled with EdU to identify replicating cells at the time of UV treatment (EdU+ cells). Four hours after UV treatment, a significant increase in ssCPD formation was observed for Polh-deficient cells and PolhMlh1-deficient cells, whereas a less pronounced increase is seen in PolhMsh6 double knockout cells (Fig. 5D-E).

Taken together these data show that the formation of ssDNA in Polh deficient cells following UV exposure is dependent on Msh6, but not on Mlh1. In line with these data, UV-induced checkpoint signaling, cell cycle arrest and apoptosis all depend on the formation of ssDNA and thus requires Msh6 to be present. In contrast, not only Msh6 suppresses UV-induced mutagenesis, but Mlh1 as well. The synergistic relationship between Polh and Msh6 suggests MMR dependent post-replicative control of TLS-errors and argues against a recruitment model. However, this control may be independent of long-lived ssDNA tracts as Mlh1 similarly suppresses TLS-associated mutagenesis but does not influence ssDNA gap formation.

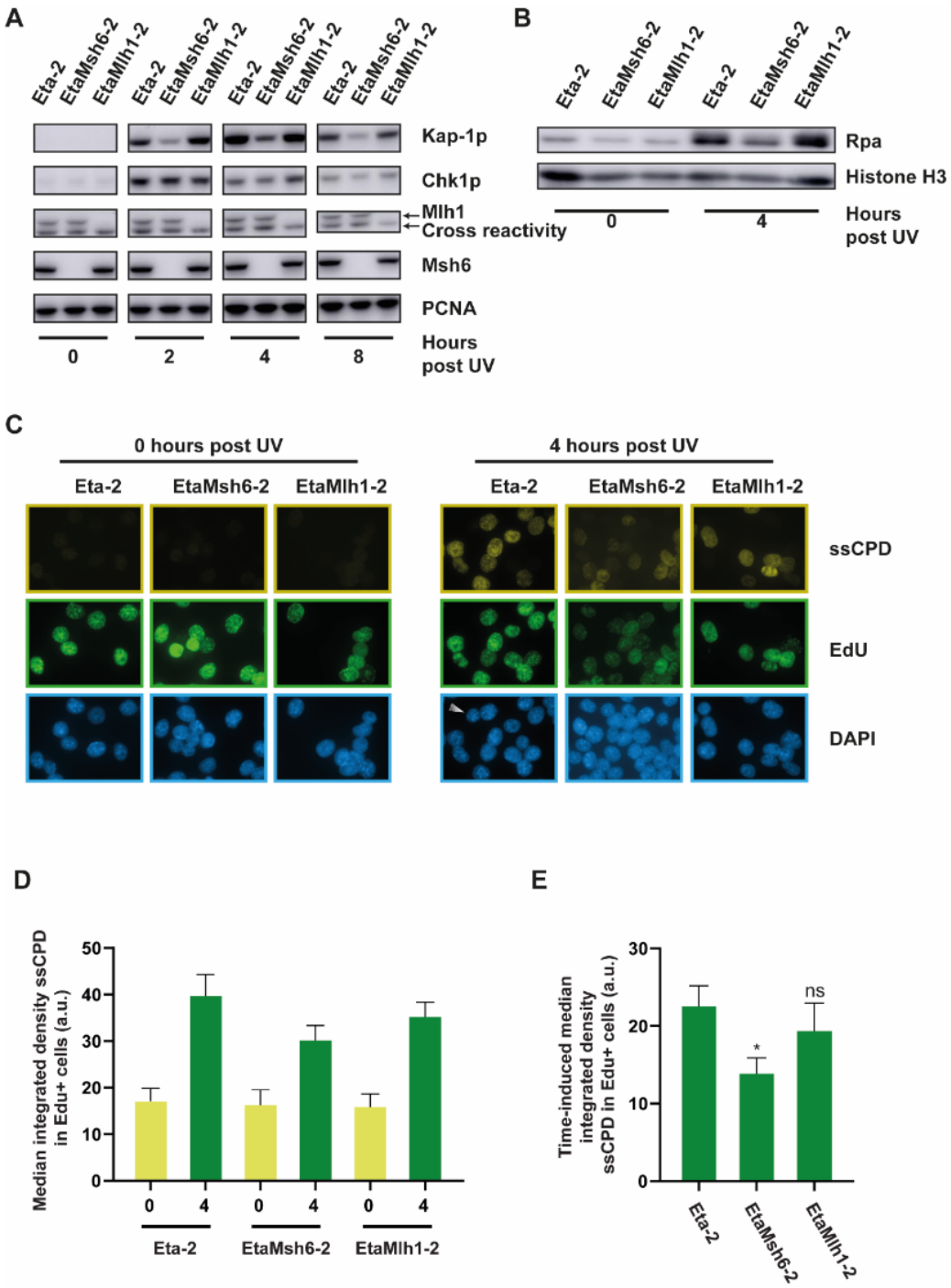

Figure 5: UV-induced checkpoint activation and ssDNA formation relies on Msh6
A: Western blots of DNA damage signaling proteins in whole protein lysates of *Polη*, *PolηMsh6* and *PolηMlh1*-deficient cells, 0-8 hours after UV exposure. Phosphorylated Chk1 and Kap-1 were assessed as a measure for ss/dsDNA break associated signaling, respectively. Antibodies against *Mlh1* and *Msh6* were used to confirm knock-out of the gene. PCNA was used as a loading control. B: Western blots of fractions of chromatin-bound proteins from *Polη*, *PolηMsh6* and *PolηMlh1* cells isolated 0 and 4 hours after UV-irradiation. Rpa was measured as a read-out for the formation of ssDNA. Histone H3 was used as a loading control. C: Immunostaining for CPD in single stranded DNA formation (ssCPD), 0- and 4-hours post-UV. EdU labeling was used to detect replicating cells at the time of UV exposure. DAPI was used as a nuclear stain. D: Quantification of the median integrated density of ssCPD in EdU+ cells. Data shown is relative to the 0 hours timepoint for each cell line. E: Normalization of the integrated density of ssCPD by subtracting the 0 hours timepoints. Error bars, IQ range; *, P ≤ 0,05; Mann-Whitney U-test of groups compared to *Polη* single mutant.

Discussion

Translesion synthesis is a DNA damage tolerance pathway that replicates damaged DNA, thereby quenching DNA damage signaling and preventing cell death at the cost of increased mutagenesis (16). Several studies indicate that DNA damage-associated mutagenesis and DNA damage signaling can be controlled by MMR (24). Two hypotheses that may explain how MMR controls DNA damage responses are (i) the recruitment of the relatively error-free Polη by MMR (19-21) or (ii) the removal of TLS-mis-incorporations known as post-TLS repair (17). Here we show that both Msh6 and Mlh1 are required to suppress UV-induced mutagenesis in *Polh*-deficient cells. Moreover, we provide evidence that presence of Msh6, but not Mlh1, further increases UV-induced ssDNA gap formation, DNA damage signaling, cell cycle responses and apoptosis in *Polh*-deficient cells. Finally, we reveal that UV-induced gap formation occurs opposite CPDs, extending previously published findings of Msh6-dependent UV-induced gap formation opposite 6-4PP (17).

We show that *Polh*-deficient mouse ES cells display increased UV-induced mutagenesis when compared to wild type cells, confirming previously published data (37). Polη replicates UV-damage efficiently and relatively error-free, due to its ability to incorporate predominantly Adenines opposite both Thymidines of a T-T CPD, the most frequently induced UV lesion by UV-C light (38, 39). In the absence of Polη, more error-prone TLS polymerases, such as polymerases kappa, iota and Rev1/Pol zeta are required for the bypass of persistent UV lesions, resulting in increased UV-induced mutagenesis and an altered spectrum of UV-induced mutations (6, 40-42). The UV mutability of *Polh*-deficient mouse ES cells is strongly affected by an additional defect in *Msh6*, since UV-induced mutagenesis in *PolhMsh6* double knockout cells is greater than the sum of UV-induced mutagenesis found in the *Polh* and *Msh6* single knockout cells. Previously, we have shown that Msh6-dependent suppression of UV-induced mutagenesis is attenuated in *Rev-1* hypomorphic cells which are hypomutable for UV (17, 43). Together, these results strongly suggest that suppression of UV-induced mutagenesis by Msh6 depends on the extent of mutagenic TLS.

Mammalian cells replicate UV-damaged DNA discontinuously by generating relatively short DNA fragments that are later converted into mature DNA molecules. This conversion is delayed in Polh-deficient cells (40, 44, 45). When a replicative DNA polymerase encounters a CPD, it is thought that a DNA polymerase switch is induced to enable Polη to bypass this lesion ‘on the fly’, i.e. direct bypass without repriming of the replication machinery downstream of the lesion (46). This mode of lesion bypass prevents the accumulation of ssDNA and overactivation of Atr/Chk1 signaling (47). Indeed, our data indicate that *Polh*-deficiency results in the generation of ssDNA tracts as shown by enhanced formation of chromatin-bound Rpa (Fig. S5) and increased levels of unreplicated CPDs in ssDNA configuration (data not shown, unable to visualize in wild-type cells), following UV exposure. This is accompanied with strongly activated UV damage signaling, confirming previous studies (47). The ssDNA tracts found in *Polh*-deficient cells might be caused by stalled forks or repriming of the

replication machinery downstream of the photolesion. This work indicates that the formation of ssDNA tracts in *Polh*-deficient cells depends partially on Msh6, since approximately half of the ssDNA gaps that are located opposite CPDs depend on Msh6 (Fig. 5C-E). In line with this, we also found that UV-induced Atr/Chk1 signaling in *Polh*-deficient cells partially depends on Msh6. Together with the important role of Msh6 in suppressing UV-induced mutagenesis in *Polh*-deficient cells, these data suggest that UV-induced Chk1 signaling relies to a certain extent on Msh6-dependent excision of TLS mis-incorporations opposite CPDs. However, prolonged stalling of replication complexes or collapsing replication forks that occur independently of Msh6 may also contribute to Chk1 activation.

In contrast to Chk1 signaling, phosphorylation of Kap1^{S824} in *Polh*-deficient cells strongly relies on Msh6. Since Kap1 phosphorylation at S824 is reported to be mediated not only by ATM and DNA-PK, but also by ATR, the formation of Kap1^{S824p} likely depends on the generation of ssDNA tracts (ATR) and of DSBs (ATM/DNA-PK) (34, 35). Consequently, Kap1 phosphorylation is associated with the activation of cell cycle arrests and apoptosis (48), which is reflected by similar responses of *Polh*-deficient cells exposed to UV (Fig. 4, S2-3). These responses are strongly reduced in *Polh*-deficient cells with an additional deficiency in Msh6. Since the formation of Kap1^{S824p} is associated with the repair of DSBs (49-51), our data may indicate that the formation of UV-induced DSBs in *Polh*-deficient cells largely depend on Msh6. Moreover, ssDNA tracts generated by Msh6-mediated excision of TLS-errors may have a higher tendency of converting into DSBs, since the more prominent role Msh6 in phosphorylating Kap1 than in the phosphorylation of Chk1.

The present study indicates that, in contrast to Msh6, Mlh1 does not play a role in the UV-induced DNA damage response in *Polh*-deficient mouse ES cells, as shown by Mlh1-independent induction of UV damage signaling, cell cycle arrests and apoptosis. However, both Mlh1 and Msh6 suppress UV-induced mutagenesis to a similar extent. These data are in line with comparable experiments performed in mouse ES cells deficient for nucleotide excision repair (NER) (Chapter 3). Based on mutation spectra analyses, these experiments suggested that both Mlh1 and Msh6 act at ‘mis-incorporations’ opposite UV damage at dipyrimidine sites, although their identity remains to be determined. As stated previously, Msh6 may act on ‘mis-incorporations’ opposite CPDs and (6-4)PPs based on immunostainings of ssCPDs (Fig. 5C-E) and ss(6-4)PPs as well as on UV mutagenesis experiments using cells that express a CPD photolyase (17). In contrast to Msh6, Mlh1 does not seem to act on ‘mis-incorporations’ opposite CPDs, since similar levels of ssCPDs were found in *Polh*-deficient mouse ES cells irrespective of Mlh1 status (Fig. 5C-E). It might be that during lagging strand synthesis a proportion of ‘mis-incorporations’ opposite CPDs are removed in an Mlh1-independent manner, as non-ligated Okazaki fragments still contain a 5’ end that allows Mlh1-independent repair. We noted that, following UV exposure, Mlh1-deficient mouse ES cells display enhanced levels of chromatin-bound Rpa (Fig. 5B, S4B), which may reflect stabilized replication forks at UV lesions. Recruitment of Rpa to stalled replication forks will deplete the pool of free Rpa, which may render cells defective in

NER (52, 53). In mouse cells, NER deficiency will affect predominantly the removal of (6-4)PPs, since CPDs are only repaired from transcribed strands of active genes (54, 55). Thus, although Msh6 and Mlh1 suppress UV-induced mutagenesis in *Polh*-deficient mouse ES cells to the same extent, they might achieve this by acting at 'mis-incorporations' opposite different subsets of UV lesions. It may be interesting to study the effect of Mlh1-deficiency in Polη-deficient cells on the formation of ssDNA gaps opposite 6-4PP.

In this study we aimed to investigate two seemingly conflicting models for the suppression of UV-induced mutagenesis by MMR proteins (Fig. 1), namely the recruitment model (19-21) and the post-TLS repair model (17). The former proposes a role for Msh6 by recruiting TLS polymerases to the replication-blocking UV lesion (epistasis), while the latter suggests a post-replicative role for MMR proteins due to the removal of erroneous TLS-incorporations (synergism). Apparently, our *Hprt* mutant frequency experiments in *Polh*-deficient cells with an additional *Msh6* or *Mlh1* deficiency contradicts the recruitment model, since defects in both TLS and MMR led to mutagenic synergism rather than epistasis. Yet, the post-TLS repair model cannot fully explain the present data, since loss of Mlh1 did not result in lower levels of UV-induced ssDNA which would be expected if Mlh1 is required to promote excision of TLS-induced 'mis-incorporations' across UV lesions. Instead, the two models may be interwoven (Fig. 6): In certain instances downstream repriming of the replication machinery causes UV-lesions to be bypassed erroneously by post-replicative gap filling by Rev1/Polζ (45). The resulting TLS-errors may be recognized and subsequently removed by the joined action of MutSα and MutLα, thus reducing mutagenesis. Following the removal, MutSα is essential to recruit relatively error-free polymerases, such as Polη, or in its absence Polκ or Polι, thereby preventing the accumulation of ssDNA and accompanied damage responses.

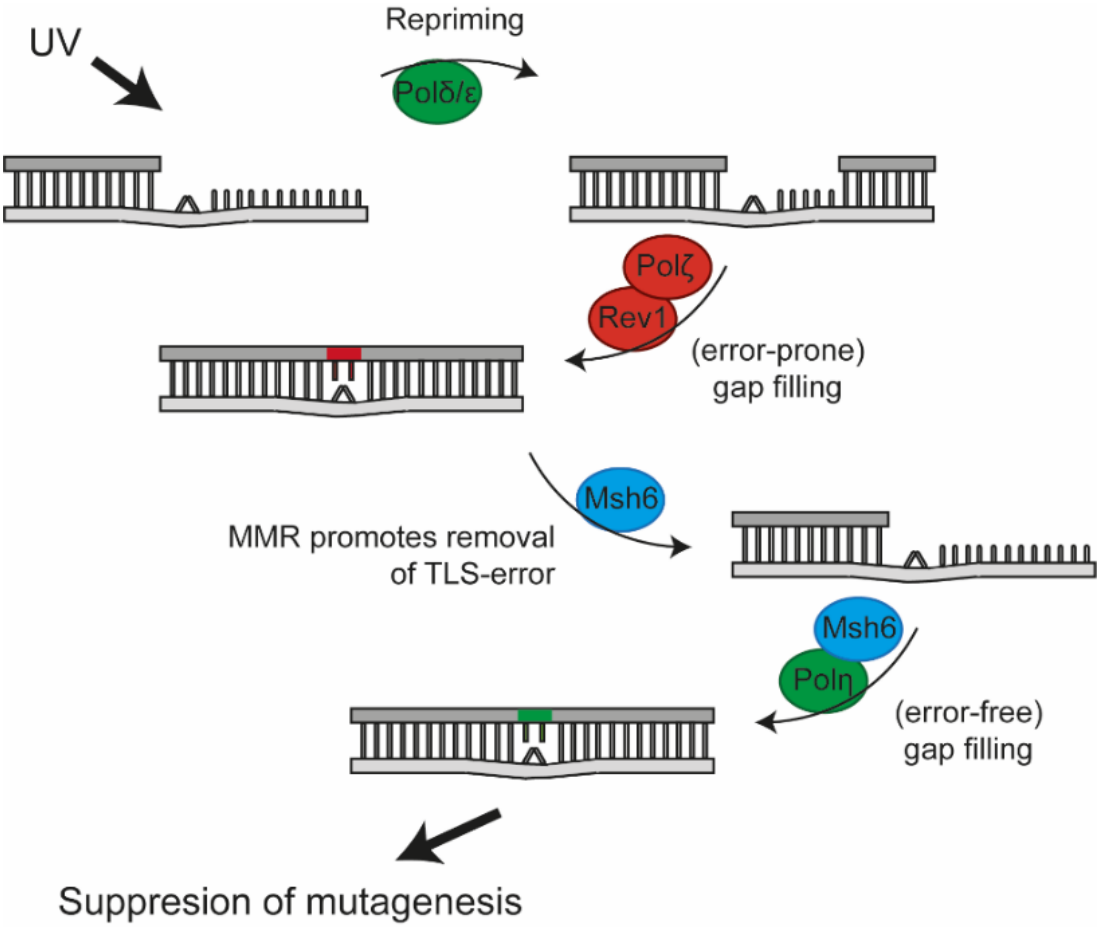

Figure 6: An integrated model where Msh6 both removes TLS errors and promotes error-free TLS
DNA exposed to UV forms intrastrand crosslinks that may sometimes cause the replication machinery to reprime downstream of the damage. For gap-filling Rev1/Polζ may be recruited which can cause TLS-errors. Msh6 is able to recognize these misincorporations opposite the damage and subsequently removes it. Afterwards Msh6 recruits the relatively error-free Polη to bypass the damage, thus suppressing UV-induced mutagenesis.

Supplemental Materials

Supplemental materials table 1: guideRNA sequences used for CRISPR

CRISPR table	*gRNA 1*	*gRNA 2*	*Target*	*Protein/mRNA*	*6tG selected*
Polη	*CGCTGTCATTGGACTCCGCC*	*GAATCATGTTGACTGCTCAA*	*Entire gene*	*No mRNA*	*No*
Msh6	*GGAGCCTCCGCTTCCCGCGG*	*CCTTTGATGGAACGTTCAT*	*Exon 1-2*	*No protein*	*Yes*
Mlh1	*CTCCTCCGGAGTGAGCACGG*	*ATGCCAGATTGGACCAACTA*	*Entire gene*	*No protein*	*Yes*

Supplemental materials table 2: PCR primer sequences

Target:	*Forward*	*Reverse*
Polη external	*AGCGTGAGTCCCAGAAGTTG*	*AGCTTGCCAGGTTCTTTATACCT*
Polη internal	*CAATGGGCTGGCAAGCTTTT*	*CAGGAGCCGCAGAGTTACTA*

Supplemental Figures

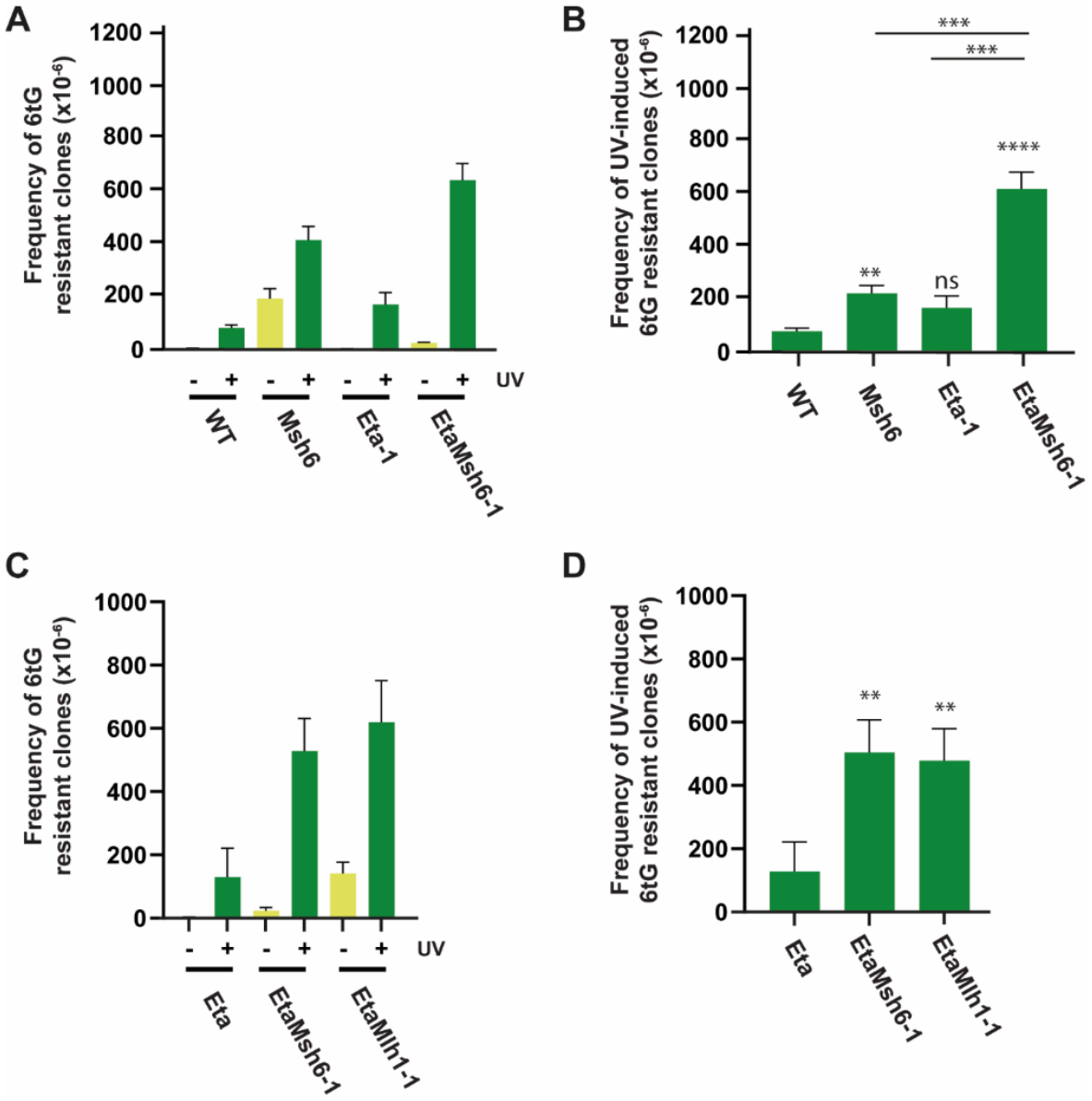

Figure S1: UV-induced mutagenesis in independent cell lines
A: Frequencies of 6tG resistant clones per million clone forming cells in mock treated and UV-exposed WT, *Msh6*, *Polη* and *PolηMsh6*-deficient cells. B: Frequencies of UV-induced 6tG resistant clones in WT, *Msh6*, *Polη* and *PolηMsh6*-deficient cells shown per million clone forming cells. C: Quantification of mutagenesis in mock and UV-conditions in *Polη*, *PolηMsh6* and *PolηMlh1*-deficient cells per million cells. D: UV-induced mutagenesis in *Polη*, *PolηMsh6* and *PolηMlh1*-deficient cells per million cells. Independent cell lines were used to validate the findings of Fig. 1. Error bars, SEM; **, P ≤ 0,01; ****, P ≤ 0,0001; ns, non-significant; student T-test of groups compared to WT or *Polη* single mutant or between Eta*Msh6* and single mutants.

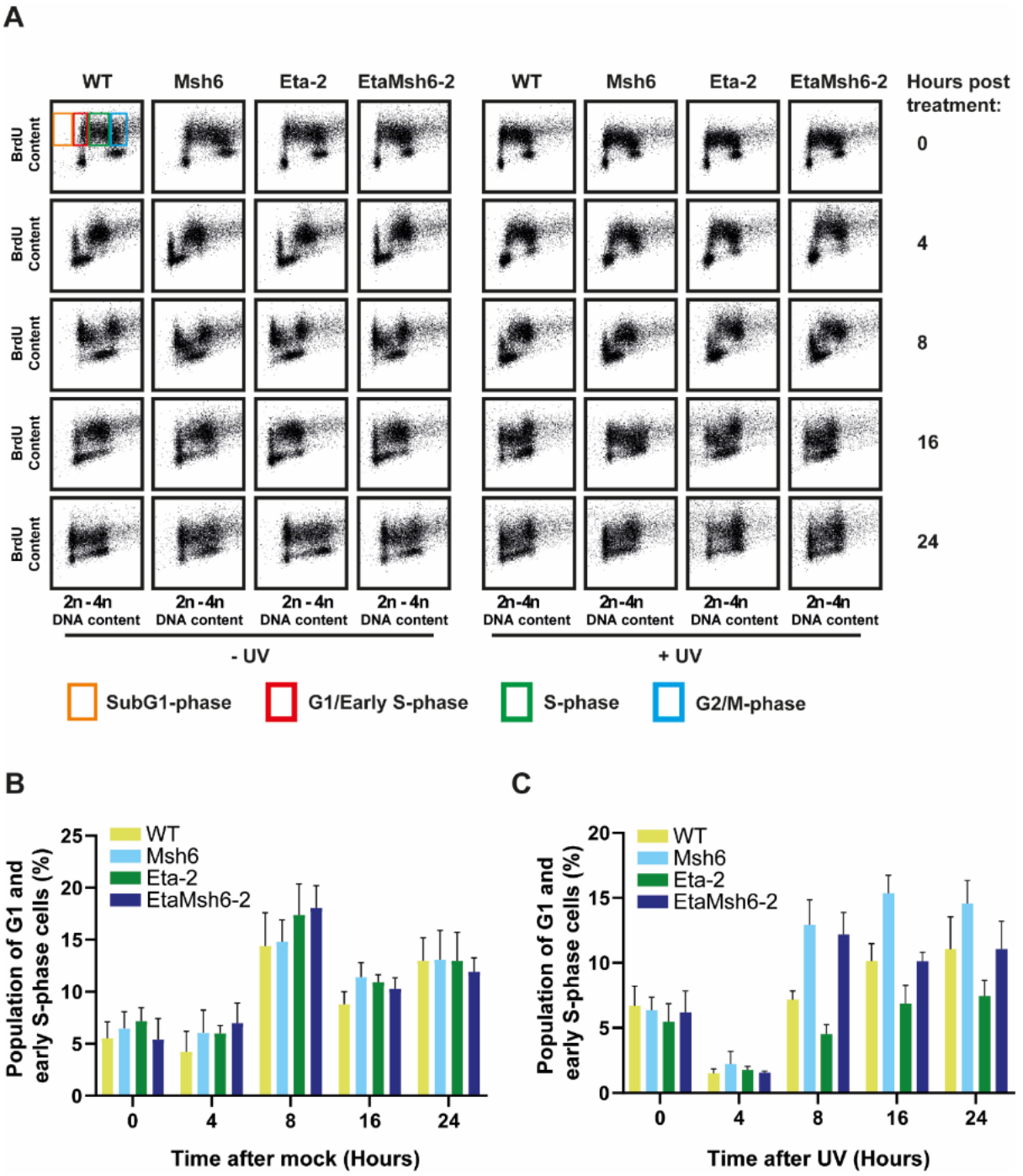

Figure S2: Cell cycle progression in WT, Msh6, Eta and EtaMsh6-deficient lines.
A: Cell cycle plots were obtained using FACS with a BRDU-FITC pulse-labeling for replicating cells plotted against total DNA content by staining with propidium iodine depicting a population of WT, *Msh6*, *Polη* and *PolηMsh6*-deficient cells 0-24 hours after mock or UV-exposure. B: Quantification of the mean population of G1/Early S-phase cells relative to the total amount of cells in WT, *Msh6*, *Polη* and *PolηMsh6*-deficient cells 0-24 hours post mock treatment. C: Quantification of the mean population of G1/Early S-phase cells relative to the total amount of cells in WT, *Msh6*, *Polη* and *PolηMsh6*-deficient cells 0-24 hours post mock treatment. Error bars, SEM.

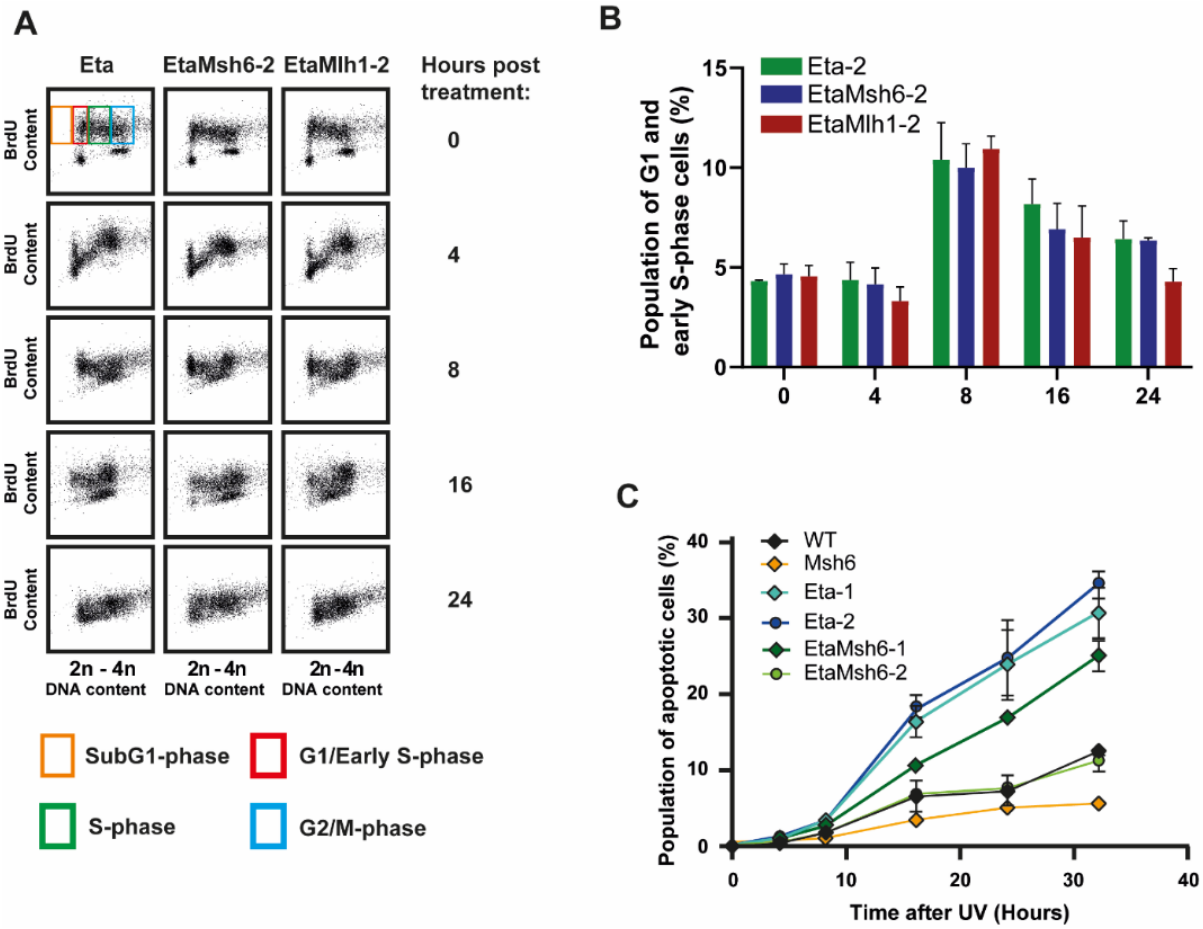

Figure S3: Cell cycle progression and apoptosis in WT, Msh6, Eta, EtaMsh6 and EtaMlh1-deficient lines. A: Cell cycle plots were obtained using FACS with a BRDU-FITC pulse-labeling for replicating cells plotted against total DNA content by staining with propidium iodine depicting a population of *Polη, PolηMsh6*, and *PolηMlh1*-deficient cells 0-24 hours after mock treatment. B: Quantification of the mean population of G1/Early S-phase cells relative to the total amount of cells in *Polη, PolηMsh6*, and *PolηMlh1*-deficient cells 0-24 hours post mock treatment. C: Quantification of the mean population of sub-G1 cells relative to the total amount of cells 0-32 hours post-UV irradiation in WT, *Msh6*, *Polη* and *PolηMsh6*-deficient conditions. Multiple lines tested to validate the results of figure 4. Error bars, SEM.

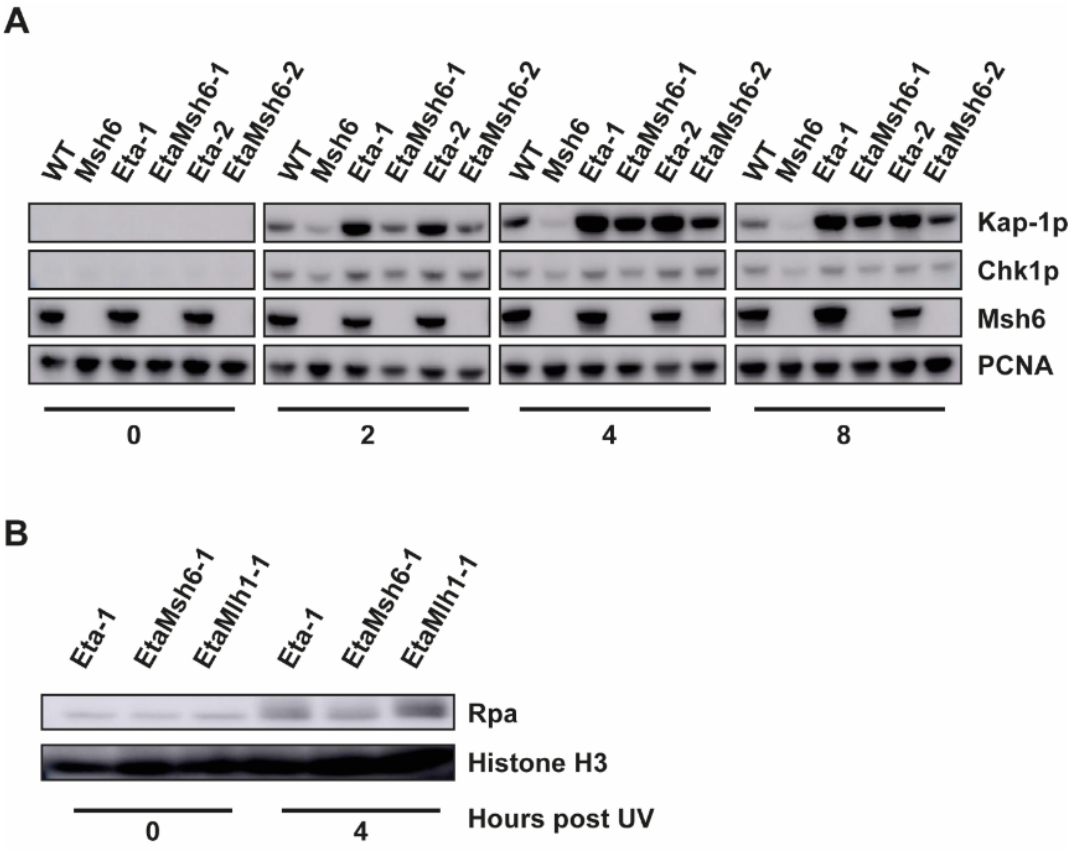

Figure S4: UV-induced DNA damage signaling and ssDNA formation in independent cell lines
A: Western blots of whole cell lysates using antibodies against phosphorylated Chk1 and Kap1. Phosphorylated Chk1 and Kap-1 were assessed as a measure for ss/dsDNA break associated signaling, respectively. Antibodies against *Msh6* were used to confirm knock-out of the gene. PCNA was used as a loading control. B: Chromatin-bound fractions of *Polη*, *PolηMsh6* and *PolηMlh1* cells were collected 0 and 4 hours after UV-irradiation. The amount of Rpa was measured as a read-out for the formation of ssDNA across the genome. Histone H3 was used as a loading control. Independent cell lines were used to validate the findings of Fig. 5.

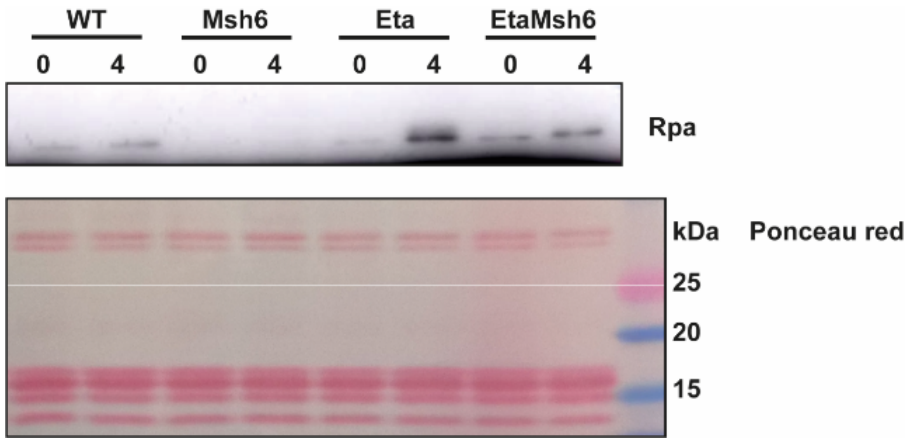

Figure S5: UV-induced ssDNA formation in independent Eta and EtaMsh6-deficient cell lines
Chromatin-bound fractions of WT, *Msh6*, *Polη and PolηMsh6* cells were collected 0 and 4 hours after UV-irradiation. Chromatin-bound Rpa as a read-out for the formation of ssDNA across the genome was determined by Western blot. Equal loading of proteins was verified by Ponceau red staining of the membrane after blotting .

References

1. Sale JE, Lehmann AR, Woodgate R. Y-family DNA polymerases and their role in tolerance of cellular DNA damage. Nature reviews Molecular cell biology. 2012;13(3):141-52.
2. Yang W, Gao Y. Translesion and Repair DNA Polymerases: Diverse Structure and Mechanism. Annual Review of Biochemistry. 2018;87(1):239-61.
3. Biertumpfel C, Zhao Y, Kondo Y, Ramon-Maiques S, Gregory M, Lee JY, et al. Structure and mechanism of human DNA polymerase eta. Nature. 2010;465(7301):1044-8.
4. Masutani C, Kusumoto R, Yamada A, Dohmae N, Yokoi M, Yuasa M, et al. The XPV (xeroderma pigmentosum variant) gene encodes human DNA polymerase eta. Nature. 1999;399(6737):700-4.
5. Gratchev A, Strein P, Utikal J, Sergij G. Molecular genetics of Xeroderma pigmentosum variant. Experimental dermatology. 2003;12(5):529-36.
6. Yoon JH, Prakash L, Prakash S. Highly error-free role of DNA polymerase eta in the replicative bypass of UV-induced pyrimidine dimers in mouse and human cells. Proc Natl Acad Sci U S A. 2009;106(43):18219-24.
7. Yang W, Gao Y. Translesion and Repair DNA Polymerases: Diverse Structure and Mechanism. Annu Rev Biochem. 2018;87:239-61.
8. Bebenek K, Matsuda T, Masutani C, Hanaoka F, Kunkel TA. Proofreading of DNA polymerase eta-dependent replication errors. J Biol Chem. 2001;276(4):2317-20.
9. Washington MT, Johnson RE, Prakash S, Prakash L. Mismatch extension ability of yeast and human DNA polymerase eta. J Biol Chem. 2001;276(3):2263-6.
10. Zhang Y, Yuan F, Presnell SR, Tian K, Gao Y, Tomkinson AE, et al. Reconstitution of 5′-Directed Human Mismatch Repair in a Purified System. Cell. 2005;122(5):693-705.
11. Wyatt MD, Pittman DL. Methylating Agents and DNA Repair Responses: Methylated Bases and Sources of Strand Breaks. Chemical Research in Toxicology. 2006;19(12):1580-94.
12. Fu D, Calvo JA, Samson LD. Balancing repair and tolerance of DNA damage caused by alkylating agents. Nature Reviews Cancer. 2012;12(2):104-20.
13. Mazurek A, Berardini M, Fishel R. Activation of Human MutS Homologs by 8-Oxo-guanine DNA Damage. Journal of Biological Chemistry. 2002;277(10):8260-6.
14. Borgdorff V, Pauw B, van Hees-Stuivenberg S, de Wind N. DNA mismatch repair mediates protection from mutagenesis induced by short-wave ultraviolet light. DNA Repair (Amst). 2006;5(11):1364-72.
15. Ijsselsteijn R, van Hees S, Drost M, Jansen JG, de Wind N. Induction of mismatch repair deficiency, compromised DNA damage signaling and compound hypermutagenesis by a dietary mutagen in a cell-based model for Lynch Syndrome. Carcinogenesis. 2021.
16. Friedberg EC. Suffering in silence: the tolerance of DNA damage. Nature Reviews Molecular Cell Biology. 2005;6(12):943-53.
17. Tsaalbi-Shtylik A, Ferras C, Pauw B, Hendriks G, Temviriyanukul P, Carlee L, et al. Excision of translesion synthesis errors orchestrates responses to helix-distorting DNA lesions. J Cell Biol. 2015;209(1):33-46.
18. Wang H, Lawrence CW, Li GM, Hays JB. Specific binding of human MSH2.MSH6 mismatch-repair protein heterodimers to DNA incorporating thymine- or uracil-containing UV light photoproducts opposite mismatched bases. J Biol Chem. 1999;274(24):16894-900.
19. Zlatanou A, Despras E, Braz-Petta T, Boubakour-Azzouz I, Pouvelle C, Grant, et al. The hMsh2-hMsh6 Complex Acts in Concert with Monoubiquitinated PCNA and Pol η in Response to Oxidative DNA Damage in Human Cells. Molecular Cell. 2011;43(4):649-62.
20. Peña-Diaz J, Bregenhorn S, Ghodgaonkar M, Follonier C, Artola-Borán M, Castor D, et al. Noncanonical Mismatch Repair as a Source of Genomic Instability in Human Cells. Molecular Cell. 2012;47(5):669-80.
21. Lv L, Wang F, Ma X, Yang Y, Wang Z, Liu H, et al. Mismatch repair protein MSH2 regulates translesion DNA synthesis following exposure of cells to UV radiation. Nucleic Acids Res. 2013;41(22):10312-22.
22. Zhang J, Zhao X, Liu L, Li HD, Gu L, Castrillon DH, et al. The mismatch recognition protein MutSalpha promotes nascent strand degradation at stalled replication forks. Proc Natl Acad Sci U S A. 2022;119(40):e2201738119.
23. Guan J, Lu C, Jin Q, Lu H, Chen X, Tian L, et al. MLH1 Deficiency-Triggered DNA Hyperexcision by Exonuclease 1 Activates the cGAS-STING Pathway. Cancer Cell. 2021;39(1):109-21 e5.
24. Ijsselsteijn R, Jansen JG, De Wind N. DNA mismatch repair-dependent DNA damage responses and cancer. DNA Repair. 2020;93:102923.
25. Stojic L, Brun R, Jiricny J. Mismatch repair and DNA damage signalling. DNA Repair (Amst). 2004;3(8-9):1091-101.
26. Smith J, Tho LM, Xu N, Gillespie DA. The ATM-Chk2 and ATR-Chk1 pathways in DNA damage signaling and cancer. Advances in cancer research. 2010;108:73-112.
27. Hooper M, Hardy K, Handyside A, Hunter S, Monk M. HPRT-deficient (Lesch-Nyhan) mouse embryos derived from germline colonization by cultured cells. Nature. 1987;326(6110):292-5.
28. Van Gool IC, Rayner E, Osse EM, Nout RA, Creutzberg CL, Tomlinson IPM, et al. Adjuvant Treatment for POLE Proofreading Domain-Mutant Cancers: Sensitivity to Radiotherapy, Chemotherapy, and Nucleoside Analogues. Clin Cancer Res. 2018;24(13):3197-203.
29. Borgdorff V, van Hees-Stuivenberg S, Meijers CM, de Wind N. Spontaneous and mutagen-induced loss of DNA mismatch repair in Msh2-heterozygous mammalian cells. Mutat Res. 2005;574(1-2):50-7.

30. Nara K, Nagashima F, Yasui A. Highly elevated ultraviolet-induced mutation frequency in isolated Chinese hamster cell lines defective in nucleotide excision repair and mismatch repair proteins. Cancer Res. 2001;61(1):50-2.
31. Glaab WE, Skopek TR. Cytotoxic and mutagenic response of mismatch repair-defective human cancer cells exposed to a food-associated heterocyclic amine. Carcinogenesis. 1999;20(3):391-4.
32. Stary A, Kannouche P, Lehmann AR, Sarasin A. Role of DNA polymerase eta in the UV mutation spectrum in human cells. J Biol Chem. 2003;278(21):18767-75.
33. Ziv Y, Bielopolski D, Galanty Y, Lukas C, Taya Y, Schultz DC, et al. Chromatin relaxation in response to DNA double-strand breaks is modulated by a novel ATM- and KAP-1 dependent pathway. Nature cell biology. 2006;8(8):870-6.
34. White DE, Negorev D, Peng H, Ivanov AV, Maul GG, Rauscher FJ, 3rd. KAP1, a novel substrate for PIKK family members, colocalizes with numerous damage response factors at DNA lesions. Cancer Res. 2006;66(24):11594-9.
35. Hu C, Zhang S, Gao X, Gao X, Xu X, Lv Y, et al. Roles of Kruppel-associated Box (KRAB)-associated Co-repressor KAP1 Ser-473 Phosphorylation in DNA Damage Response. J Biol Chem. 2012;287(23):18937-52.
36. Wang Y, Qin J. MSH2 and ATR form a signaling module and regulate two branches of the damage response to DNA methylation. Proc Natl Acad Sci U S A. 2003;100(26):15387-92.
37. Maher VM, Ouellette LM, Curren RD, McCormick JJ. Frequency of ultraviolet light-induced mutations is higher in xeroderma pigmentosum variant cells than in normal human cells. Nature. 1976;261(5561):593-5.
38. Johnson RE, Prakash S, Prakash L. Efficient bypass of a thymine-thymine dimer by yeast DNA polymerase, Poleta. Science. 1999;283(5404):1001-4.
39. Washington MT, Johnson RE, Prakash S, Prakash L. Accuracy of thymine-thymine dimer bypass by Saccharomyces cerevisiae DNA polymerase eta. Proc Natl Acad Sci U S A. 2000;97(7):3094-9.
40. Jansen JG, Temviriyanukul P, Wit N, Delbos F, Reynaud CA, Jacobs H, et al. Redundancy of mammalian Y family DNA polymerases in cellular responses to genomic DNA lesions induced by ultraviolet light. Nucleic Acids Res. 2014;42(17):11071-82.
41. Ziv O, Geacintov N, Nakajima S, Yasui A, Livneh Z. DNA polymerase zeta cooperates with polymerases kappa and iota in translesion DNA synthesis across pyrimidine photodimers in cells from XPV patients. Proc Natl Acad Sci U S A. 2009;106(28):11552-7.
42. Wang Y, Woodgate R, McManus TP, Mead S, McCormick JJ, Maher VM. Evidence that in xeroderma pigmentosum variant cells, which lack DNA polymerase eta, DNA polymerase iota causes the very high frequency and unique spectrum of UV-induced mutations. Cancer Res. 2007;67(7):3018-26.
43. Jansen JG, Tsaalbi-Shtylik A, Langerak P, Calleja F, Meijers CM, Jacobs H, et al. The BRCT domain of mammalian Rev1 is involved in regulating DNA translesion synthesis. Nucleic Acids Res. 2005;33(1):356-65.
44. Lehmann AR, Kirk-Bell S, Arlett CF, Paterson MC, Lohman PH, de Weerd-Kastelein EA, et al. Xeroderma pigmentosum cells with normal levels of excision repair have a defect in DNA synthesis after UV-irradiation. Proc Natl Acad Sci U S A. 1975;72(1):219-23.
45. Temviriyanukul P, van Hees-Stuivenberg S, Delbos F, Jacobs H, de Wind N, Jansen JG. Temporally distinct translesion synthesis pathways for ultraviolet light-induced photoproducts in the mammalian genome. DNA Repair (Amst). 2012;11(6):550-8.
46. Edmunds CE, Simpson LJ, Sale JE. PCNA ubiquitination and REV1 define temporally distinct mechanisms for controlling translesion synthesis in the avian cell line DT40. Mol Cell. 2008;30(4):519-29.
47. Despras E, Daboussi F, Hyrien O, Marheineke K, Kannouche PL. ATR/Chk1 pathway is essential for resumption of DNA synthesis and cell survival in UV-irradiated XP variant cells. Human molecular genetics. 2010;19(9):1690-701.
48. Li X, Lee YK, Jeng JC, Yen Y, Schultz DC, Shih HM, et al. Role for KAP1 serine 824 phosphorylation and sumoylation/desumoylation switch in regulating KAP1-mediated transcriptional repression. J Biol Chem. 2007;282(50):36177-89.
49. Goodarzi AA, Noon AT, Deckbar D, Ziv Y, Shiloh Y, Lobrich M, et al. ATM signaling facilitates repair of DNA double-strand breaks associated with heterochromatin. Mol Cell. 2008;31(2):167-77.
50. Iyengar S, Farnham PJ. KAP1 protein: an enigmatic master regulator of the genome. J Biol Chem. 2011;286(30):26267-76.
51. Kuo CY, Li X, Stark JM, Shih HM, Ann DK. RNF4 regulates DNA double-strand break repair in a cell cycle-dependent manner. Cell cycle. 2016;15(6):787-98.
52. Tsaalbi-Shtylik A, Moser J, Mullenders LH, Jansen JG, de Wind N. Persistently stalled replication forks inhibit nucleotide excision repair in trans by sequestering Replication protein A. Nucleic Acids Res. 2014;42(7):4406-13.
53. Auclair Y, Rouget R, Belisle JM, Costantino S, Drobetsky EA. Requirement for functional DNA polymerase eta in genome-wide repair of UV-induced DNA damage during S phase. DNA Repair (Amst). 2010;9(7):754-64.
54. Ruven HJ, Berg RJ, Seelen CM, Dekkers JA, Lohman PH, Mullenders LH, et al. Ultraviolet-induced cyclobutane pyrimidine dimers are selectively removed from transcriptionally active genes in the epidermis of the hairless mouse. Cancer Res. 1993;53(7):1642-5.
55. Mitchell DL. The relative cytotoxicity of (6-4) photoproducts and cyclobutane dimers in mammalian cells. Photochemistry and photobiology. 1988;48(1):51-7.